Room temperature fabrication of 1D carbon-copper composite nanostructures directly on Cu substrate and their field emission properties

Mohamad Saufi Rosmi,[1,2,a] Yazid Yaakob,[1,3] Mohd Zamri Mohd Yusop,[4] Subash Sharma,[1] Zurita Zulkifli,[5] Aizuddin Supee,[6] Golap Kalita,[1] and Masaki Tanemura[1]

[1]*Department of Frontier Materials, Nagoya Institute of Technology, Gokiso-cho, Showa-ku, Nagoya 466-8555, Japan*
[2]*Department of Chemistry, Faculty of Science and Mathematics, Universiti Pendidikan Sultan Idris, 35900 Tanjong Malim, Perak, Malaysia*
[3]*Department of Physics, Faculty of Science, Universiti Putra Malaysia, 43400 UPM Serdang, Selangor, Malaysia*
[4]*Department of Materials, Faculty of Mechanical Engineering, Universiti Teknologi Malaysia, 81310 Skudai, Johor, Malaysia*
[5]*Faculty of Electrical Engineering, Universiti Teknologi Mara, Malaysia*
[6]*Faculty of Chemical and Energy Engineering, Universiti Teknologi Malaysia, 81310 Johor Bahru, Johor, Malaysia*

(Received 25 May 2016; accepted 6 September 2016; published online 13 September 2016)

This paper demonstrates a carbon-copper (C-Cu) composite nanostructure directly fabricated on a copper (Cu) substrate using the Ar^+ ion irradiation method at room temperature. The morphology of C-Cu composite was controlled by a simultaneous carbon supply during ion irradiation. Conical protrusions formed on the surface of the Cu substrate with the low carbon supply rate (R_C), whereas high R_C area prominently produced nanoneedle structures. The field electron emission (FEE) tests demonstrated significant improvement between conical protrusions and nanoneedle structures, where the emission current increase from 5.70 μAcm^{-2} to 4.37 $mAcm^{-2}$, while the turn-on field reduced from 5.90 to 2.00 $V\mu m^{-1}$. © *2016 Author(s). All article content, except where otherwise noted, is licensed under a Creative Commons Attribution (CC BY) license (http://creativecommons.org/licenses/by/4.0/).* [http://dx.doi.org/10.1063/1.4962971]

Currently, one-dimensional (1D) carbon nanostructure materials, namely nanowires, nanotubes and nanofibers have attracted great deal of attention due to its extraordinary structure, high aspect ratio, and excellent electrical and mechanical properties.[1–3] The overwhelming attention promoted interests in composite structure with various metals.[4,5] The motivation of the interests is a result of the tunable characteristics and promising applications of 1D nanostructure materials in various fields, including as field electron emission (FEE) emitter.[6,7] To date, various techniques have been explored to synthesize carbon-metals composites including arc discharge, chemical vapor deposition (CVD) and high temperature pyrolysis.[8–11] However, all these methods require temperature of higher than 500 °C, which sometimes leads to a serious drawback for practical application. In order to be viable for commercial usage, synthesis methods at lower temperature, ideally at room temperature is essential.

Previously, ion irradiation method was employed to synthesize carbon nanofibers (CNFs) either on the carbon or carbon coated metal substrates, without the need for catalyst even at room temperature.[4,12–14] This method has been proven to be effective for carbon nanostructure fabrication that contains metal or metal carbide. Favorably, various kinds of carbon-metal composite nanostructures such as nanofibers, nanoneedles and nanocones could grow when the substrates were irradiated by an

[a]Corresponding author: E-mail: (M. S. Rosmi) saufirosmi@gmail.com; Phone/Fax: +81-52-735-5379

ion beam with inert gases and simultaneous metal supply.[15–18] In this regard, room temperature ion irradiation growth of carbon-metal composite nanostructures directly on conductive metal substrate enables the tailoring of composite nanostructure according to the application requirement.

The advantages of direct growth of carbon-metal composite nanostructure on conductive metal substrate are twofold, namely (i) minimize the contact resistance between nanostructures and the conductive substrate; and (ii) providing good bonding between nanostructures and the substrate.[19–21] These advantages is believed to improve the FEE properties. It is widely known that the morphology of nanomaterials severely influences its own properties and applications. The geometrical and chemical elements, namely emitter size, aspect ratio, composition and numerical density significantly affect the FEE properties.[22–24] Hence, this technique was expanded to reveal the formation of carbon-copper (C-Cu) composite nanostructure with various morphologies and FEE properties.

Cu possesses excellent thermal and electrical conductivities.[25] The combination of Cu and C will be fascinating for various applications such as FEE devices. However, the apparent interface between 1D carbon nanostructure and Cu substrate is not preferable for this application because the interface is in general weak mechanically and electrically. The seamless configuration of 1D nanostructure and substrate will be promising for the applications. Very unfortunately, this goal is difficult to achieve for pure carbon, namely 1D carbon nanostructure on Cu substrate. By contrast, for 1D C-Cu composite nanostructure, this seamless structure fabrication can be easily achievable by the ion irradiation method. So, our expectation is to achieve the seamless structure for 1D C-Cu composites nanostructure with keeping both Cu concentration as high as possible and controllability of 1D structure as much as possible. Therefore, in this paper, we carried out the morphological and compositional controls of C-Cu composite nanostructures, which are grown directly on a Cu substrate at the room temperature without any catalyst. Furthermore, in this paper, the applicability of this nanostructure as a FEE emitter for future (FEDs) is also investigated.

The samples employed in this experimental work were commercially available Cu substrate with a thickness of 0.2 mm. The C-Cu composite nanostructures were grown on the Cu substrate with a size of 25 x 10 x 0.2 mm^3. Cu substrate was mounted on a sample stage and a graphite plate (C wall) acting as the carbon atom supplier was placed perpendicular to the edge of the Cu substrate (Figure 1(a)). Ion irradiations onto Cu substrate and C wall at 1 keV were performed at the room temperature for 60 minutes by using Kaufman type ion gun with the ion beam diameter of 6 cm (ION TECH. INC Ltd., model 3-1500-100FC). Ion incident angle was 45° with respect to the normal surface for both Cu substrate and C wall. The basal and working pressures for C-Cu composite nanostructures fabrication were 1.5 x 10^{-5} and 2 x 10^{-2} Pa, respectively. The etching rate of Cu was 68.8 nm/min, almost independent of the area. The C supply rate (R_C) were 0.17, 0.67, 0.83, 1.67 and 2.83 nm/min, depending on the distance from the C wall (Table I). To determine the Rc, C wall, which was placed perpendicular to SiO_2 (300 nm in thickness) covered Si platelet(SiO_2/Si), 1.0 x 2.5 cm^2 in size, was irradiated by Ar^+ under the same ion irradiation condition as that for the fabrication of C-Cu composite nanostructure for 60 minute. As seen in the figure 1(b) below, in order to avoid the ion irradiation onto SiO_2/Si substrate, protection wall (C) was also placed at the other

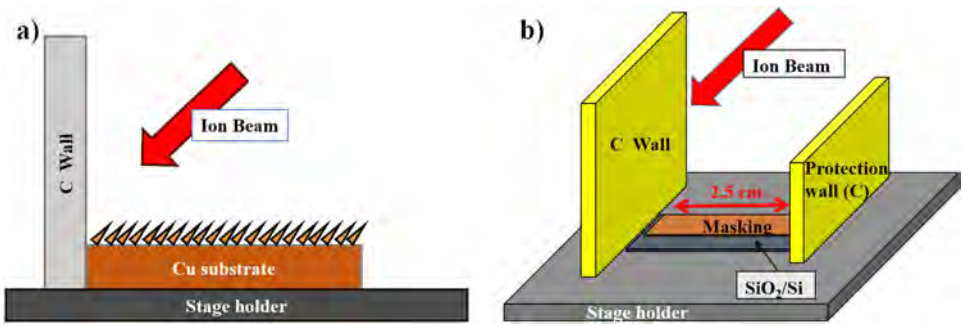

FIG. 1. (a) Schematic illustration of experimental arrangement used to fabricate C-Cu composite nanostructure. (b) Schematic illustration of experimental arrangement used to deposit carbon onto SiO_2/Si.

TABLE I. R_C at different distance from C wall.

Distance from C wall (cm)	C supply rate, Rc (nm/min)
2.5	0.17
2.0	0.67
1.5	0.83
1.0	1.67
0.5	2.83

front edge of the SiO_2/Si substrate. The deposition area was fixed to 0.5 cm x 2.5 cm by masking SiO_2/Si and the thickness of C film deposited was measured by a profile meter Surfcom-1400D (Accretech-Tokyo Seimitsu). The Rc then was calculated by using equation (1) as shown below as a function of the distance from the carbon wall:

$$\text{Carbon supply rate} = \frac{\text{Carbon film thickness (nm)}}{\text{deposition time (min)}} \quad (1)$$

After ion beam irradiation, scanning electron microscopy (SEM, JEOL JEM-5600) and transmission electron microscopy equipped with energy dispersive X-ray (EDS) (TEM; JEOL JEM-2010HR) were used for the observations of the morphologies of the sample surfaces and the crystalline structure of C-Cu composite nanostructures, respectively. For FEE measurements, a parallel plate configuration was used under vacuum condition of 3×10^{-4} Pa. An ITO-coated glass was used as an anode, whereas a cathode (C-Cu composite nanostructures) was separated from the anode by utilizing a Teflon spacer with 100 μm thickness. The size of the emission area is 0.1 cm^2, with applied voltage ranging from 0 and 1000 V to characterize the FEE behavior.

Figures 2(a)-(e) illustrate the SEM images of the Cu surfaces sputtered with simultaneous supply of C at R_C of 0.17, 0.67, 0.83, 1.67 and 2.83 nm/min. The SEM images clearly indicate that the morphology of C-Cu composite nanostructures highly depends on the R_C. The surfaces with low level of C supply (R_C= 0.17 and 0.67 nm/min) experienced relatively high density of conical protrusions of 5 x 10^3 mm^{-2} [Figure 2(a) and 2(b)]. It is observed that the conical protrusions are pointing toward the direction of ion beam, while no needle-like nanostructure formed on the protrusions. It is unveiled

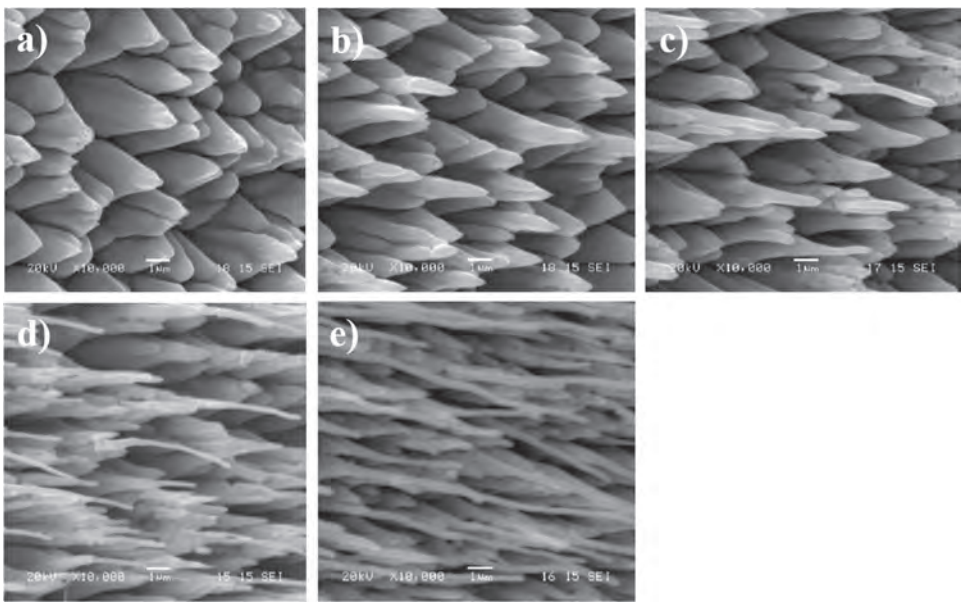

FIG. 2. SEM images of sputtered Cu substrate with a simultaneous C supply rate (R_C) of (a) 0.17 (b) 0.67 (c) 0.83 (d) 1.67 and (e) 2.83 nm/min.

that the irradiated surface with R_C of 0.67 nm/min [Figure 2(b)] exhibits an extended length of conical protrusions compared to surface with R_C of 0.17 nm/min [Figure 2(a)]; 2.5 and 1.5 μm, respectively. For the case of surface sputtered with moderate R_C [R_C= 0.83 nm/min; Figure 2(c)], short C-Cu nanoneedles start to grow on several conical protrusions, which were on average 2.5 μm in length, 0.2 μm in width, and 3 x 10^3 mm^{-2} in density respectively. Further increase in the R_C yielded high density of lengthy C-Cu nanoneedle structures [R_C= 1.67 and 2.83 nm/min; Figures 2(d) and 2(e)]. Additionally, it is found that the C-Cu nanoneedle structures formed during the higher R_C is longer compared to the C-Cu form at moderate R_C with length of 5.0-8.5 μm and diameter of 0.1 μm. Note that, with increasing of R_C, the number density of C-Cu nanoneedle was increased from 4 x 10^3 mm^{-2} to 4.6 x 10^3 mm^{-2}. It is noted that there is very less conical protrusions without the C-Cu nanoneedle observed at the area with high R_C.

As is well-known, surface diffusion of C plays important role in the CNF growth.[13] Similar to this CNF growth, the surface diffusion of carbon is thought to be responsible for the C-Cu nanostructure formation. The formation mechanism of the ion induced C-Cu composite nanostructure would be the re-deposition of sputter ejected Cu and C atom onto the side wall of conical protrusions and the surface diffusion of the re-deposited Cu and C atoms towards the tips during the ion irradiation process. Therefore, at the low C supply region, erosion process is more dominant than the growth process resulting in no needle formation. This hypothesis is in line with the morphologies of the C-Cu nanostructure formed at the region with higher R_C, where the longer C-Cu nanoneedles were formed.

The composition of C-Cu composite nanostructure is confirmed by the EDS analysis, as shown in Table II. It is clear that only Cu and C were detected with various percentages. The C concentration in C-Cu composite nanostructures is linearly proportional to the R_C (refer Tables I and II). The crystallite structures of the C-Cu composite nanostructures with different R_C are further investigated using TEM, as depicted in Figures 3(a)-(d). For C-Cu conical protrusions grown with R_C of 0.17 nm/min, only small amount of C layer covered the polycrystalline Cu protrusions [Figure 3(a)], consistent with EDX result which showed that the conical protrusions consist of 6% of C and 94% of Cu. For the surface with R_C of 0.67 nm/min [Figure 3(b)], the C-Cu conical protrusions formed consist of C coated Cu crystallites with slightly higher C concentration. The aforementioned result is established via EDS analysis, which revealed that the structure consists of 89% Cu and 11% C. In the case of C-Cu nanoneedle structure grown at the R_C higher than 0.83 nm/min, no boundary between the nanoneedle structure and the cone was recognizable [Figure 3(c)]. For further clarification, the TEM image revealed that the Cu nanoparticles are homogenously distributed along the structure of the C-Cu nanoneedle structures. The EDS analysis revealed that the C-Cu nanoneedle structures consist of Cu and C at 87% and 13%, respectively. In Figure 3(d), the image depicts the selected area electron diffraction (SAED) pattern of C-Cu composite nanoneedle, which consists of a broad ring with several spots. Through a careful analysis, the inner ring and the spots thereon are able to be identified as graphite (002) and polycrystalline Cu (111), Cu (220), Cu (200) and Cu (311).

The C-Cu composite nanostructures grown directly on the Cu substrate with various R_C are studied for FEE properties as shown in Figure 4. The turn on field, defined as the field required to extract a current density of 1 nA/cm^2, is 8.0 and 5.9 V/μm for the emitter grown at lower R_C [R_C =0.17 and 0.67 nm/min]. For the emitter grown at lower R_C [R_C=0.17 and 0.67 nm/min], the threshold fields relative to the current density of 0.1μA/cm^2 are 9.8 and 7.2 V/μm, respectively. In the case of the C-Cu nanoneedle structure grown at moderate R_C [R_C=0.83 nm/min], the turn on field

TABLE II. Percentage of C and Cu dependence on the R_C.

C supply rate, R_C (nm/min)	Percentage of C (%)	Percentage of Cu (%)
0.17	6	94
0.67	11	89
0.83	13	87
1.67	20	80
2.83	22	78

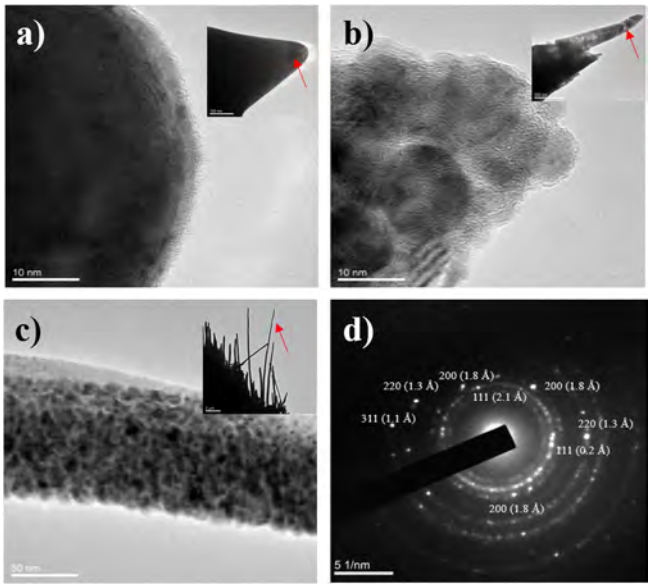

FIG. 3. TEM images of Cu substrate with a simultaneous C supply rate (R_C) of (a) 0.17 (b) 0.67 (c) more than 0.83 nm/min, (d) SAED of C-Cu composite nanostructure.

and threshold voltage are 3.0 and 5.2 V/μm, respectively. The turn on fields for C-Cu nanoneedle structure grown with high R_C (R_C = 1.67 and 2.83 nm/min) are 2.0 and 3.2 V/μm. Meanwhile, the threshold fields are 4 and 5.6 V/μm for the C-Cu nanoneedle structure grown at high R_C. It can be seen that the emitter grown with R_C of 0.17, 0.67 and 0.83 nm/min exhibits maximum current densities of 0.3, 5.7 and 28 μA/cm^2, respectively. The C-Cu nanoneedle emitter grown with higher R_C demonstrates significant and high current densities of 4.37 and 1.3 mA/cm^2. The current-voltage (I-V) curves were analyzed using a Fowler-Nordheim (F-N) plot (inset in Figure 4) to determine the field enhancement factor (β), with an assumption that the work function of C-Cu composite structure is to be 4.65 eV.[26] The β calculated from the slopes of the F-N plots for the emitter with R_C=0.17, 0.67, 0.83, 1.67 and 2.83 nm/min were 317, 514, 540, 8455 and 1918, respectively.

There seems to be no field emission at the electric field (E) values lower than ~ 9.0, 7.7, 5.5 and 5.0 V/um (corresponding to ~0.11, 0.13, 0.18 and 0.20 um/V in F-N plot) for Rc of 0.17, 0.67,

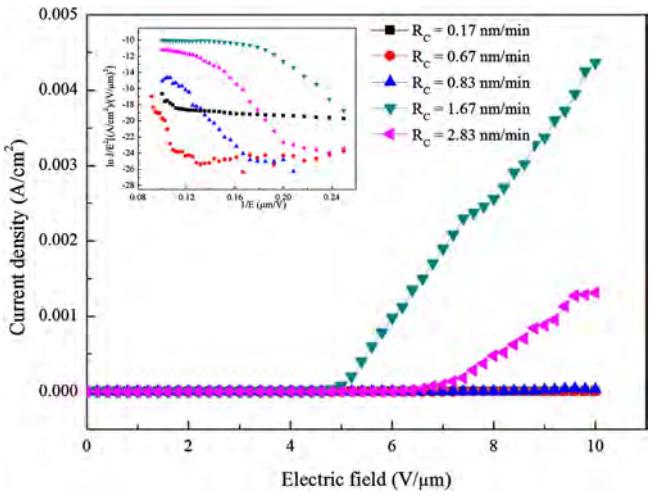

FIG. 4. Current-voltage characteristic for the C-Cu composite nanostructures. Applied voltage was 0-1000 V with an increasing step of 20 V.

TABLE III. Dependence of the geometrical structure, apex radii, average length and numerical density on the Rc.

Rc (nm/min)	Geometrical structure	Apex radii (μm)	Length (μm)	Density (mm^{-2})
0.17	Conical protrusion	2.0	1.5	5.0×10^3
0.67	Conical protrusion	0.5	2.5	5.0×10^3
0.83	Short nanoneedle	0.2	2.5	3.0×10^3
1.67	Long nanoneedle	0.1	8.5	4.0×10^3
2.83	Long nanoneedle	0.1	8.5	4.6×10^3

0.83, and 2.83 nm/min, respectively. Table III summarizes the dependence of the numerical density, average length and apex radii on the Rc. It should be noted that long C-Cu nanoneedles with small apex possess high current densities and high β. Smaller apex radii of emitters would create high effective local electric field at the respective tips resulting in high FEE current. It should be also noted that FEE property is better for Rc of 1.67 nm/min than for Rc of 2.83 nm/min. This would be because the field strength at the respective tip decreased due to higher numerical density (namely closer spacing between the neighboring nanoneedles) for Rc of 2.83 nm/min, which is known as screening effect. In fact, D. Nicolaescu *et al.* demonstrated that the fibers can be considered as 'noninteracting' only if the half-distance between adjacent fibers is about five times their height for the regular array of vertically aligned fibers.[27] In addition, F-N plots for C-Cu nanoneedles for Rc of 2.83 nm/min and of 1.67 nm/min did not show the straight lines, in which at higher electric field the FEE property gradually decreased. This would be also due to the space charge effect at high current density at confined emission area.[28]

In conclusion, we have demonstrated the morphological control of C-Cu composite nanostructures on highly conductive Cu substrate at room temperature without any catalyst. The research was conducted by simultaneously supplying C on the Cu substrate at room temperature by using the ion irradiation method. The morphology and FEE properties of the C-Cu composite nanostructure were thoroughly investigated. Conical protrusions were formed on Cu surface with low R_C, whereas those surface with high R_C produced nanoneedles. Thus, the structure and morphology of the C-Cu composite nanostructure on large area conductive substrate is controllable by adjusting the R_C, leading to a significant improvement in the FEE properties.

[1] S. Bhanushali, P. Ghosh, A. Ganesh, and W. Cheng, Small **11**, 1232 (2015).
[2] S. S. Madani, K. Zare, M. Ghoranneviss, and A. Salar Elahi, J. Alloys Compd. **648**, 1104 (2015).
[3] M. Tanemura, T. Okita, H. Yamauchi, and S. Tanemura, Appl. Phys. Lett. **84**(19), 3831 (2004).
[4] Y. Yaakob, Y. Kuwataka, M. Z. Mohd Yusop, S. Tanaka, M. S. Rosmi, G. Kalita, and M. Tanemura, Phys. Status Solidi B **252**(6), 1345 (2015).
[5] X. Qi, J. Xua, Q. Hu, W. Zhong, and Y. Du, Mater. Sci. Eng. B **198**, 108 (2015).
[6] J. Y. Pan, Y. L. Gao, and C. F. Yang, Microelectron. Eng. **148**, 34 (2015).
[7] A. B. Suriani, R. N. Safitri, A. Mohamed, S. Alfarisa, I. M. Isa, A. Kamari, N. Hashim, M. K. Ahmad, M. F. Malek, and M. Rusop, Mater. Lett. **149**, 66 (2015).
[8] O. Łabędz, A. Grabias, W. Kaszuwara, and M. Bystrzejewski, J. of Alloys Compd. **603**, 230 (2014).
[9] H. Zhang, C. Liang, J. Liu, Z. Tian, and G. Shao, Carbon **55**, 108 (2013).
[10] C. Cui, W. Qian, C. Zheng, Y. Liu, S. Yun, Y. Yu, J. Nie, and F. Wei, Chem. Engin. J **223**, 617 (2013).
[11] M. Chen, L. Bin, S. Huai-he, and Z. Lin-jie, New Carbon Mater. **25**(3), 199 (2010).
[12] D. Takeuchi, Z. P. Wang, A. Miyawaki, K. Yamaguchi, Y. Suzuki, M. Tanemura, Y. Hayashi, and P. R. Somani, Diamond Relat. Mater. **17**, 581 (2008).
[13] Z. Wang, M. Z. Mohd Yusop, T. Hihara, A. Hayashi, Y. Hayashi, and M. Tanemura, Appl. Surf. Sci. **256**, 6371 (2010).
[14] Y. Yaakob, M. Z. Yusop, C. Takahashi, G. Kalita, P. Ghosh, and M. Tanemura, Jpn. J. Appl. Phys. **52**, 11NL01 (2013).
[15] M. Zamri, P. Ghosh, Z. P. Wang, M. Kawagishi, A. Hayashi, Y. Hayashi, and M. Tanemura, J. Vac. Sci. Technol. B **28**(2), 9 (2010).
[16] A. Miyawaki, M. Zamri, T. Hayashi, Y. Hayashi, M. Tanemura, and T. Tokunaga, Surf. Coat. Technol. **206**, 812 (2011).
[17] Z. Wang, Z. Yusop, P. Ghosh, Y. Hayashi and M. Tanemura, Appl. Surf. Sci. **257**, 3168 (2011)
[18] G. K. Wehner, J. Vac. Sci. Technol. A **3**, 1821 (1985).
[19] A. M. Rao, D. Jacques, R. C. Haddon, W. Zhu, C. Bower, and S. Jin, Appl. Phys. Lett. **76**(25), 3813 (2000).
[20] I. Lahiri, R. dan Seelaboyina, J. Y. Hwang, R. Banerjee, and W. Choi, Carbon **48**, 1531 (2010).
[21] P. Ghosh, M. Zamri Yusop, D. Ghosh, A. Hayashi, Y. Hayashi, and M. Tanemura, Chem. Commun **47**, 4820 (2011).
[22] A. B. Suriani, A. R. Dalila, A. Mohamed, I. M. Isa, A. Kamari, N. Hashim, T. Soga, and M. Tanemura, Mater. Res. Bull. **70**, 524 (2015).
[23] Y. Ling-min, F. Xin-hui, Q. Li-jun, and Y. Wen, Appl. Surf. Sci. **257**, 6332 (2011).

[24] P. Mahanandia, V. Arya, P. V. Bhotla, S. V. Subramanyam, J. J. Schneider, and K. K. Nanda, Appl. Phys. Lett. **95**, 083108 (2009).
[25] L. Lu, Y. Shen, X. Chen, L. Qian, and K. Lu, Science **304**, 422 (2004).
[26] S. Talapatra, S. Kar, S. K. Pal, R. Vajtai, L. Ci, P. Victor, M. M. Shaijumon, S. Kaur, O. Nalamasu, and P. M. Ajayan, Nat. Nanotechnol **1**, 112 (2006).
[27] D. Nicolaescu, V. Filip, and F. Okuyama, J. Vac. Sci. Technol. A **15**(4), 2369 (1997).
[28] A. Rokhlenko, K. L. Jensen, and J. L. Lebowitz, J. Appl. Phys. **107**, 014904 (2010).